Temporal Study of Urban Growth and Land Surface Temperature Extraction: A Study of the Klang Valley area

Illyani Ibrahim
Department of Urban Regional Planning, Kuliyyah of Architecture and Environmental Design, International Islamic University Malaysia (IIUM), Gombak, Selangor
Illyani_i@iium.edu.my

Azizan Abu Samah
Department of Geography, Faculty of Arts and Social Sciences, University of Malaya, Kuala Lumpur
azizans@um.edu.my

Rosmadi Fauzi
Department of Geography, Faculty of Arts and Social Sciences, University of Malaya, Kuala Lumpur
rosmadifauzi@um.edu.my

ABSTRACT

The expansion of urbanization has received much attention since the late 19th century. A physical aspect that needs to be understood is the urban climate problem such as the urban heat island phenomenon and its factors and effects towards environment. The steady economic growth and rapid urbanization has created more concrete landscapes that can increase the level of discomfort for the population especially in the Klang Valley region. The problem is worsening in the Klang Valley area which is plagued by extensive economic activities and the heat generated from factories, transport and air conditioners. As such, this study examines the expansion of urban growth and the temporal pattern of the land surface temperature which has influenced the quality of air quality. This study utilizes the Landsat images for different time periods and unsupervised classification had been carried out to retrieve the land cover types. In order to isolate effects of urbanization on surface temperature, the comparison of the historical datasets of air temperature in rural and urban areas are studied. This image was processed for appropriate atmospheric and geometric correction and the extraction of land surface temperature by using the model of the mono-window algorithm. Our findings show that the rate of urbanization of the study area is 37.725 km square per year. Next, this study also shows that the urban areas have extensively expanded more than thrice in 1999 compared to 1989. Further finding of this study is that two greenery areas have a higher average temperature. However, future study will look at the main concern of the key factors can be applied by the local urban planning authority in applied climatology and remote sensing study.

Keywords: Land surface temperature, urban growth, urban heat island

1. INTRODUCTION

The expansion of impervious surface by transforming of green and natural area has receive interest from many researchers of its impact towards local and global environment. Understanding of land cover change over the period is crucial in improving land use planning and policy.

Nearly half of the world's population (47 per cent) now lives in urban areas and it is expected to grow by 2 per cent per year during 2000-2015 while it is projected to increase to nearly 5 per cent in 2030 (United Nations Population Division, 2001). Record prepared by United Nation Statistics Division (2012) shows that the urban population in Malaysia is 73.5% from the total population. Hence the comfort and the quality of environment in the urban area is an important aspect that needs to be considered.As detailed studies of UHI can be done using in-situ measurements, satellite imagery are also an effective tool to retrieve the Land Surface Temperature (LST) (Pongrácz, Bartholy et al. n.y.). The LST indicated the level of at-satellite thermal infrared radiation which also called as Surface Urban Heat Island (SUHI). Identification and characterization of UHI are typically based on land surface temperature (LST) that varies spatially, due to the complexity of land surface cover and other atmospheric factors (Joshi and Bhatt 2012). The urbanization has rapidly changing the thermal characteristic of the impervious surface area, that has significantly can be supported by the heat image produced by remote sensing imagery.

Roth (2012) had concluded that the studies of UHI in the tropical region is underrepresented. It was aware that most of the studies are written in the native language and is not published in international journal. The local study in the earlier time has shown that the in-situ measurement and meteorological data are mostly used (Sani 1990, JPBD 2002). Only in the recent studies have used remote sensing imagery (Mega and Pedersen 1998, Asmala Ahmad and Noorazuan Hashim n.y., Kubota and Ossen n.y.), however no local UHI study done by using air plane, due to the cost limitation.

Several local studies have been identified in the UHI subject. Sani (2002) is the earliest scholar that has discussed of the UHI effect to the urbanization in the study area. These studies discussed on the remote sensing method in order to retrieved the LST (Wai, Camerlengo et al. 2005, Narimah Samat 2006, Shaharuddin Ahmad and Noorazuan Md Hashim 2007, Shaharuddin Ahmad, Noorazuan Md. Hashim et al. 2009, Asmala Ahmad and Noorazuan Hashim n.y.). In addition, these authors has analysed a climatic condition in using long observation datasets gathered from Meteorology department (Sani 1990, Burghardt, Katzschner et al. 2010). However, none of them integrate the study of remote sensing image and long observational datasets of temperature to investigate how the warming rate of urban and rural differ between each other.

Ahmad Fuad Embi and Norlida Mohd Dom (n.y.) had discussed that the heat in Kuala Lumpur is not normal when compared with lesser-developed areas of the country, by observing of the city is humid (mostly above 80% humidity) even without the additional vapour. (Kubota and Ossen n.y.) found that the temperature

drops by 1 - 2º Celsius due to the existence of the green areas. Since earlier study, Sani (1990) had already identified that the gaps of urban climate and planning and management of the urban environment, and proposed to compare similar research with other temperate region. However, several parameters such as climates, weather and location need to be rely on the experimental work applied in the study area, specifically in the tropical area condition. In addition, several studies had discussed that the UHI had increased the extreme frequent rainfall and thunderstorm (Burghardt, Katzschner et al. 2010, Ahmad Fuad Embi and Norlida Mohd Dom n.y.). The argument by Shaharuddin Ahmad, Noorazuan Md. Hashim (2009) raised issue of increased of temperature is synonym with the urbanization due to the climate of hot and humid throughout the years. However, analysis done by Dizdaroglu, Yigitcanlar et al. (2010) shows reversed, where the temperature increased need to be focused more for the human comfort in the city.

The review of UHI intensity calculation using remote sensing show several methods have been implemented by different authors. These studies (Klysik and Fortuniak 1999, Xie, Guan et al. 2005) used the difference urban and rural to calculate the UHI intensity. Chen, Zhao et al. (2006) has calculated difference urban and water, (Kim and Baik 2002, Liu, Ji et al. 2007, Fung, Lam et al. 2009) used the difference of weather station in urban and rural. Lastly, (Streutker 2003, Hung, Uchihama et al. 2006) had used Gaussian approximation calculate UHI intensity.

The aim of this paper is focuses on the monitoring of the spatial and temporal pattern of UHI and the land cover influence in the Klang Valley area by utilizing Landsat datasets. Two objectives are; i) to analyse on the temporal study on the LST pattern and urban growth and ii) to analyse on the UHI among land cover types. It was aware that the Landsat images are not available from the same year, due to most of the datasets are influenced by the clouds and haze. Therefore, this study is focus on the relative temperature rather than the absolute temperature. The understanding of land cover is crucial to study the pattern of temperature distribution and the UHI effect. Finally, the influence of the urbanization growth to the urban heat island is also discussed in this study.

2. STUDY AREA

The Klang Valley is experiencing the fastest development and urbanization growth in Malaysia. This valley faces serious environmental problems such as urban heat islands, traffic congestion, air pollution from industrial and vehicular emissions and flash floods. The Klang Valley city center is located at 3°8′00″N 101° 42′00″E. Fig. 1 shows the Klang Valley area that is considered in this research. The study area comprises of urban and rural areas within Kuala Lumpur and Selangor, all which are regarded to be appropriate for this study on thermal behaviour. This urban area has fast expanded as various effects of human activities have influences the urban environment in term of the air quality and human comfort. This area is located near to the equator in the tropical area of hot and humid for entire years, which has faces two types of monsoonal season, rainy season

(northeastern monsoon) and hot season (southwester monsoon). This study area has an average annual rainfall amount of 2500 mm. The monsoon variation is give a different outcome to temperature and precipitation; as the dry monsoon would allow the precipitation to decrease and therefore warming up the temperature. However, mean range of temperature of dry and wet monsoon not give an obvious change of the temperature, as extreme as the temperate climate zone.

Figure 1 The Klang Valley region in purple

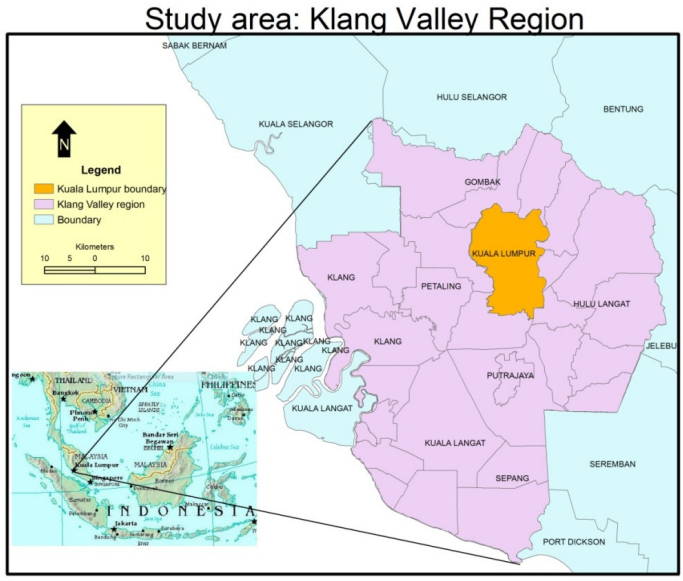

Fig. 1 had shown the Klang Valley area as the whole region, whereas this valley has seven council authorities with different policies. Kuala Lumpur, as the federal capital of Malaysia is located in the orange boundary. In the inset map (right) show the Asia boundary where Kuala Lumpur, Malaysia is located. The land cover and LST maps covers the whole region of Klang Valley including Kuala Lumpur City Center.

3. DATA AND METHODS

The Landsat image was used to calculate the land surface temperature and landcover classification by using the Erdas Imagine software package. From the areas chosen; there are four (4) temporal periods of Landsat data; Feb 1989, Feb 1999, May 2001 and Mar 2006. The correction of emissivity and the atmospheric corrections are critical in order to get appropriate results of the LST retrieval. Fig. 2 shows the method used in the study.

Figure 2 Method used in the analysis

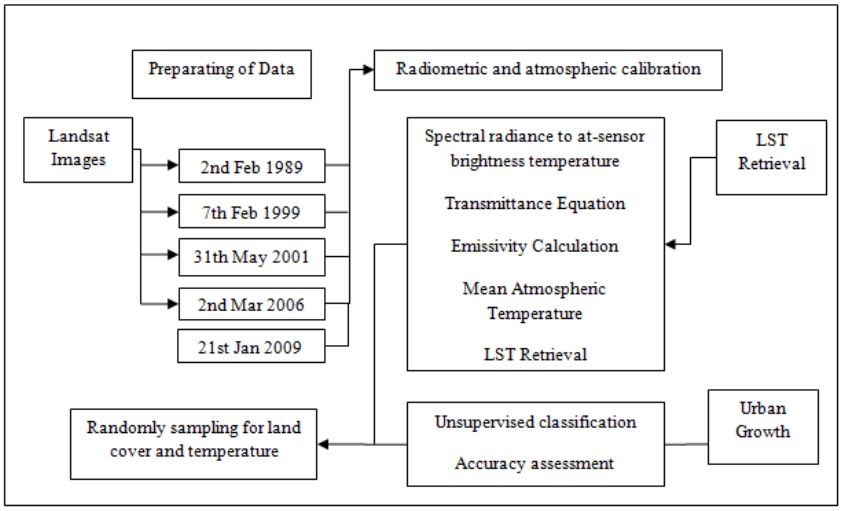

3.1 Preparation of Data.

The cloudless images were selected in order to avoid the bias of the temperature readings due to the influence of cloud that will naturally give a lower temperature. Therefore, three Landsat images were downloaded from the United States Geological Survey (USGS) under 10% of cloud with Universal Transverse Mercator (UTM) Projection. The Landsat TM images have seven bands with band 6 being the thermal infrared band of 60 meter spatial resolution while the other bands are 30 meter. The image was radiometric and geometrically corrected with the operation of the subset procedure as the process of "cropping" or cutting out a portion of an image. The details of the images are as Table 1 as below;

Table 1 Acquisition Date of the Landsat imageries

Acquisition Data	Image	Time
7th Feb 1989	Landsat 4	2:44 pm
12th Dec 1999	Landsat TM	3:03 pm
31th May 2001	Landsat ETM+	3.00 pm
2nd Mar 2006	Landsat TM	3:19 pm
21st Jan 2009	Landsat TM	3:13 pm

3.2 Radiometric and atmospheric calibration

The atmospheric effect needs to be corrected to remove the effects of atmosphere on the radiation by using the exact period of the sun elevation angle and sun-earth distance during the satellite image passage by its path in the study area. In order to remove this effect, the algorithm of COST without Tau (Dark Object Subtraction) method (WWF Malaysia 2001) was applied using the Spatial Models used in the Erdas Imagine software.

Several parameters need to be calculated before the COST formula is to be applied. For each Landsat 4 and TM images, the gains, biases and sun

elevations are provided in the metadata that accompanies the image. The sun-earth distance can be retrieved from the online (National Aeronautics and Space Administration 2012). The computation to from digital number (DN) to radiance is as follows;

$$L = Lmin\lambda + Lmax\lambda - \frac{Lmin\lambda}{(255-1)} * DN \quad (1)$$

Where λ is the ETM/TM band number, L is at sensor radiance in watts, Lmaxλ and Lminλ can be retrieved from the histogram statistics under the Layer Info menu. For Landsat 4, these attributes are prepared in the metadata together with the image. The exo-atmospheric reflectance at satellite temperatures, total Julian days, sun elevation angle and sun-earth distance for each scene were derived by from (Markham and Barker 1986) for converting DN to at-satellite reflectance. Details of images are as shown in Table 2.

Table 2 Details of images metadata

Date	Image	Total Julian Days	Sun elevation	Sun-earth distance
2nd Feb 1989	Landsat 4	38	49.95	0.98628
12th Dec 1999	Landsat TM	246	50.144	0.97832
31st May 2001	Landsat ETM+	151	57.422	1.0139
02nd Mar 2006	Landsat TM	91	56.638	0.99108
21st Jan 2009	Landsat TM	21	55.323	0.91112

3.3 LST Retrieval

The next steps that need to be performed is to compute the land surface temperature; (1) by computing the transmittance equation, (2) correcting the spectral emissivity, (3) mean atmospheric temperature and (4) land surface temperature calculation by using the method developed by (Qin and Karnieli 2001, Qin, Karnieli et al. 2001).

The spectral radiances (L) were converted into the temperature brightness (Tb).

$$Tb = K2/(\ln\frac{K1}{L} + \quad (4)$$

where K1 and K2 is a constant at 666.09 (w*m -2 *sr -1 *μm-1) and 1287.71 for Landsat ETM+, while 607.09(w*m -2 *sr -1 *μm-1) and 1260.56 for Landsat TM respectively. 0.95 indicated as the emissivity of the vegetated surfaces.

2. Transmittance Equation Computation

Calculation of atmospheric transmittance was derived by using two steps. First, the value of water vapor needs to be estimated. The variables used in the calculation of water vapor value are near surface air temperature (To) and the relative humidity (RH). The near surface air temperature were extracted from Department of Meteorology and Department of Environment. Water vapor value was estimated by equation (Li 2006) as below;

$$w^i = 0.0981 \times \left\{10 \times 0.6108 \times \exp\left[\frac{17.27\times(T_o-273.15)}{237.3+(T_o-273.15)}\right] \times RH\right\} + 0.1697 \quad (5)$$

Secondly, the equation (6) for the atmospheric transmittance (Qin and Karnieli 2001) as below;

$$\tau_6 = 1.031412 - 0.11536w \quad (6)$$

Where the estimation of atmospheric transmittance (τ_6) is depends on the water vapor content. Table 3 shows the detail values for the calculations of transmittance computation.

3. Emissivity Calculation

NDVI need to be retrieved in order to calculate the emissivity. NDVI is the vegetation index which ranges from -1 to +1, -1 usually is a water body and +1 is dense vegetation. The bare soil usually takes place at +0.1 to +0.3 which also depends on the features type.

$$NDVI = (\rho 2 - \rho 1) / (\rho 2 - \rho 1), \quad (7)$$

where $\rho 2$ is the near infrared band and $\rho 1$ is the red band of the image.

Before carrying out an emissivity calculation, the percentage of vegetation within a pixel, needs to be calculated, as indicated by Carlson and Ripley (1997). According to Sobrino, Jime´nez-Mun˜oz et al.(2004) the NDVImin is 0.15 and the NDVImax is 0.9.

$$pv = (NDVI - NDVImin)/(NDVImax - NDVImin)^2 \quad (8)$$

The emissivity can be calculated by referring to the equation produced by Sobrino, Jime´nez-Mun˜oz et al. (2004);

$$\varepsilon_6 = 0.004pv + 0.986 \quad (9)$$

4. Mean Atmospheric Temperature

Ta represents the mean atmospheric temperature in the tropical region given by the formula $Ta = 17.9769 + 0.91715\ (To)$ where To is the near surface temperature (Table 3). There is also Ta equations for other regions that can be retrieved from (Sun, Tan et al. 2010) and (A-Du, Yun-Hao et al. 2006). To is gathered from the mean ambient temperature by referring to the date and hourly record for simultaneous capture during the time the *satellite Landsat* overpasses the *area of study*. *Ta was converted to Kelvin to ensure that the calculation is valid.*

Table 3 The mean temperature for each datasets

Acquisition Date	Temperature T_0 (K)
7/2/1989	298.717 K
12/12/1999	297.066 K
31/5/2001	298.717 K
2/3/2006	298.533 K
21/1/2009	299 K

5. Land Surface Temperature Retrieval

The brightness temperature needs to be corrected based on the radiance transfer equation, which states that the sensor-observed radiance is impacted by the atmosphere and from the emitted ground (Qin, Karnieli et al. 2001).

$$Ts = [a_6(1 - C_6 - D_6) + (b_6(1 - C_6 - D_6) + C_6 + D_6)T_6 - D_6T_a]/C_6 \quad (10)$$

$$C_6 = \tau_6\varepsilon_6 \quad (11)$$

$$D_6 = (1 - \tau_6)[1 + \tau(1 - \varepsilon_6)] \quad (12)$$

where T_6 is the at-sensor brightness temperature derived from the Plank function. According to Qin and Karnieli (2001), the coefficient of parameter T_6 in accordance to the temperature ranges between 20° - 50°, a_6 = -67.9542, b_6 = +0.45987. τ_6 and ε_6 is the atmospheric transmittance and emissivity at band 6, respectively.

3.4 Preparation of Image Data for Land cover Map

Land cover maps were produced by using the Unsupervised Classification by the iteration of the clustering algorithms. Series of classes are produced to determine the signature of each class so each of the pixels is compared to these signatures and labeled with the most similar values digitally. The calculation will identify which cell location is attached to which cluster. The images were categorized into six (6) classes, including: urban areas, green areas, forest land, water bodies, bare land and clouds. Originally, the unsupervised classification was divided into fifty clusters and classified according to the analyst experience in the study area.

The calibration of the land cover and land surface temperature is carried out to ensure the accurateness of the image, therefore accuracy assessment process was critical for a land cover classification. Overall accuracy and the Kappa statistics were derived from the error matrices.

3.5 UHI and Land Cover Change

A 10000 pixel points was randomly sampling of different areas are classified according its average and land cover. A land cover types and LST was converted to pixel to perform a pixel-based overlay analysis. This area is selected based on several criteria; those areas need to have no clouds and contains different types land cover types. Mean temperature of the land cover types was calculated by averaging the temperature of each pixel for each selected sample area. Due to the monsoon and atmospheric conditions differences of each image, the absolute analysis will not taken into consideration as the UHI intensity of each images will be the focus in this research.

The statistical analysis between different groups of land cover was done. The descriptive analysis, one way ANOVA table and the post hoc analysis (Tukey test) was also carried out for proving statistical significance of the groups. The one way analysis of variance (ANOVA) is used to determine whether there is any significant difference between two groups. Dependent variable is surface temperature and the independent variable is the land cover types.

4.0 RESULTS

The result will described in detail on the urban growth and LST pattern of the available remote sensing imagery in the study area. However, the LST pattern cannot be simply be compared among different image, as parameters during the imageries captured are different in term of monsoon and atmospheric variation. Therefore, this analysis will discuss on the relative temperature rather to absolute temperature. In addition, the UHI intensity are also calculated using remote sensing method as long as observation of the meteorological data climatic. The MET datasets are also gathered using long climatological datasets from the same urban and rural dataset to identify the urban heat island growth over the time.

4.1 Urban growth and LST pattern

Urban growth (Fig. 3) and land surface temperature (Fig. 4) extraction are presented. Accuracy assessment were carried out for these images and the overall accuracy and overall Kappa coefficient, respectively are gathered; Feb 1989 (93.33%, 0.9204), Dec 1999 (96.4%, 0.9580), 2001 (85.4%, 0.8299) and 2006 (85%, 0.82), show a good accuracy were achieved for the land cover classification.

Figure 3 Urban Growth according years studied

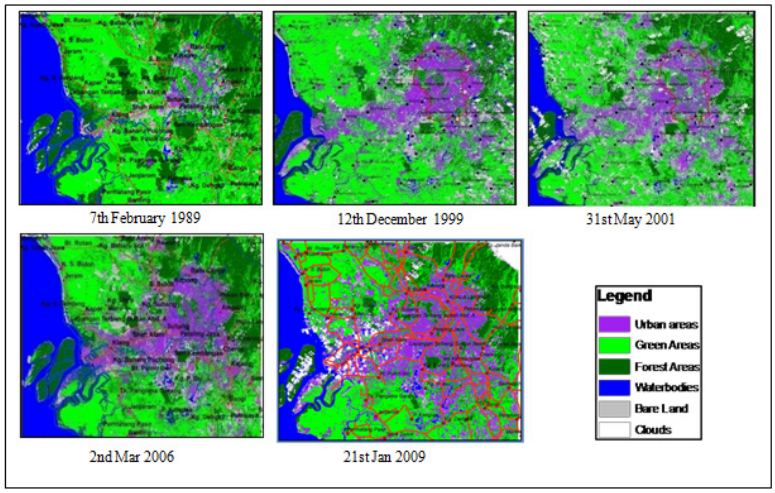

5- 6 November 2014, One Helang Hotel, Langkawi / eISBN 9789670314198

Figure 4 LST pattern according years studied

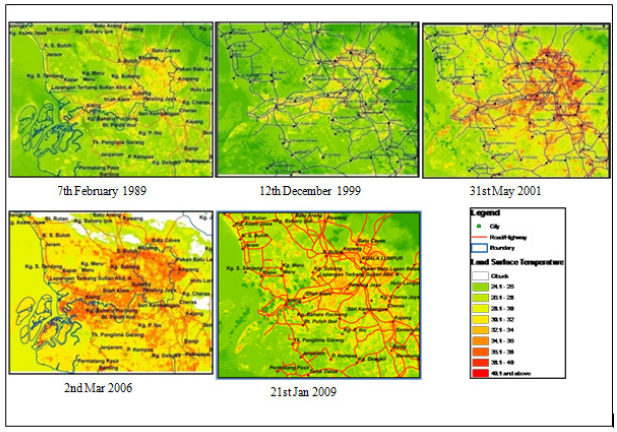

The urbanization have extended from the Northeast to the Southwest up to the coastal area from 1989 to 1999. After a decade, the expansion was not only focused on the South West of the coastal area, but it also went as far as the Northwest and Southeast areas (Feb 1999 and May 2001). The pattern of urbanized areas has transformed from the linear pattern by examining on the 1989 image. The linear pattern continuously aggregrated in 2006 image, which show a dramatic expansion of urban area in the Klang Valley region. The urban areas had been found to be denser in both directions. Referring to these maps, the pattern of urban sprawl is linear with topography in the east forming a physical barrier to the exposure, as was seen by dense forested in the image at the north east.

Table 4 Areas (in km²) of the land cover types according images

Land cover	Feb 1989	Dec 1999	May 2001	Feb 2006	Jan 2009
Urban Area	184.643	758.926	759.031	788.081	832.66
Green Land	1904.214	1674.632	1429.453	891.883	870.122
Forest Land	1323.587	967.878	908.658	908.185	907.231
Water bodies	126.668	125.360	124.062	119.938	119.144
Bare Land	341.634	385.232	257.336	408.500	355.123

By examining at Table 4, the transition statistic shows the percentage of each forest area changing to the urban area in the duration from 1989 to 2009. By using percentage wise, the findings show that the urban area has increased significantly from only 13% to 16% after 10 years, 17% in 2001 and enlarged to 18% in the next six years ahead. The other land cover types; green area, forest and waterbodies are decreasing over time to give space to urban areas to be developed. The analysis found that the rate of urbanization spreads is 37.725 km per year.

The maps provided shown that the higher temperature is manifest in the

urban areas, while lower temperature was found in the green areas. Urbanization has altered ground surfaces to a non-evaporating and non-transpiring surface of concrete and paved surfaces, which subsequently have altered energy balance in the urban areas. The development of green areas or forest areas to developed areas, which is increasing the proportion of impervious surface has increasing temperature as well, as the linearly correlation was found between these variables. The asphalt and concrete plays a role as a good heat absorber which has encourage higher temperature in such areas.

Amongst these images, the same LST pattern are found to be concentric and linearly distributed, which agreed with the land cover distribution with extreme temperatures, to be found in the urbanized area (darkest red) and it is overwhelmed by the high temperatures while the upper areas with forests with lower temperature (lightest red). It can be seen that the temperature decreases gradually from the urban area to the rural areas; whereby this goes to prove that urban heat island does exist in the study area.

Another finding in this research is regarding the greenery areas. According to 2nd Mar 2006 image, an unexpected result was recorded at Datuk Keramat Lake Park where a higher temperature has occurred with an average temperature of 38° Celsius. The same result was also found in Manjalara Lake Park (average temperature of 35° Celsius). Both parks have their own lake but still have a higher temperature. The same pattern of higher temperature in these two parks was also true to the other images. This finding lead to another published study on the contributed biophysical factors in greenery area (Ibrahim, Abu Samah et al. 2013).

Table 5 Extracted multiple comparison result of Tukey's test (º C)

Table 5 shows the statistical analysis using multiple comparison using Tukey's test for each imagery. Generally, 21st Jan 2009 images has the lowest difference among the land cover types which confirms that this image was has the lowest UHI intensity (among the other images). However, 31st May 2001 has the highest UHI intensity compared to the other images.

The difference of urban and the other land cover types (or UHI) are calculated; which show that built up area has the highest mean temperature compared to the other land cover types. Amongst every land cover, water has much difference with built-up compared to the other land cover. This is probably due to the high capacity of water to lower or increasing heat from the surrounding. On the other hand, bare land has less temperature difference compared to the other land cover types. It may be due to the fact that most of the bare land is the land for ongoing development and it has no vegetation cover.

The observation of this research shown that not necessary those urban area can have a high temperature. The maps suggest that the areas with relatively high temperatures are urban and bare land areas while those greenery,

5- 6 November 2014, One Helang Hotel, Langkawi / eISBN 9789670314198

forest and waterbodies plays a role as a moderator temperature has slightly lower temperature. The centers of high temperatures mostly located in residential areas (36%) and highway/road areas (29%) by referring to the land use map.

This analysis summarises that the temperature variation is different according to the land cover types, which urban area is the highest while the waterbodies as the lowest temperature. This is supported of the water body heat capacity which is higher compared to the land area and needs more energy to heat it up compared to the same amount of land and it takes longer time (Ibrahim, 2011). The urban area has driven by several factors that had increased the temperature such as human activities. Non-vegetated impervious surfaces of extensive constructions would store huge quantities of solar radiation and re-radiated in urban areas (Nonomura et al, 2009). However, climatic analysis also need to be taken into account for the validation of the land surface temperature imagery analysis.

Image date	Built up - green	Built up – forest	Built up-water	Built up - bare land
7th Feb 1989	3.1970212	3.7155477	5.6639775	2.3361592
12th Dec 1999	2.6922965	3.7308335	4.3715081	1.3355427
31st May 2001	3.8512781	5.0642039	5.0574798	2.0806553
2nd Mar 2006	3.1724010	3.8549802	5.6817823	1.2480222
21st Jan 2009	1.0820321	2.5495631	2.7190316	.4903053
Average	2.47695288	3.5467716	4.36826056	1.32908946

5. CONCLUSIONS

From the above analysis, five different conclusions can be derived from remote sensing imageries in LST image analysis and land cover map; LST land cover pattern throughout the years studied, UHI intensity, greenery pattern and the urban growth pattern. The findings include the five points as shown below;

1. LST pattern is concentric and linearly distributed. Higher LST follows the transportation network within the city (roads and highways).

2. A consistent pattern of UHI was shown between the available images. The snapshot of UHI can be seen from spatial dataset from earlier images to the last one. It started from Kuala Lumpur and has emerged through the highway linkages. However, high LST have accumulated at the north of the Kuala Lumpur area (e.g. Sentul, Ampang and Batu Caves) and at the Klang area, which are largely industrial areas.

3. Not every park has a capacity to moderate temperature. Some of them contain higher temperatures compared to industrial areas, for example, Manjalara Lake Garden and Datuk Keramat Lake Garden.

4. It was shown that the forest and green areas have the potential to lower

temperatures. However, the decreasing pattern of the forest and green land which have been converted to urban and bare land is indirectly leading to deterioration of the environment.

5. Some bare land shows higher LST in the urban area and this is attributed to the type of soil, where mostly it is newly developed areas containing a very high absorption capacity of soil, or it can be due to less evaporation.
6. UHI intensity is not depends on urbanization alone, but it is depends on the weather.

5- 6 November 2014, One Helang Hotel, Langkawi / eISBN 9789670314198

6. REFERENCES

A-Du, G., C. Yun-Hao, L. Jing, G. Hui-Li and L. Xiao-Juan (2006). Spatial distribution patterns of

the urban heat island based on Remote Sensing images: A case study in Beijing, China. Geoscience and Remote Sensing Symposium, 2006. I GARSS 2006. IEEE International Conference on.

Ahmad Fuad Embi and Norlida Mohd Dom (n.y.). “Urban heat islands effects on the microclimate of Malaysian cities.”

Asmala Ahmad and Noorazuan Hashim (n.y.). “A remote sensing-GIS evaluation of urban growth-land surface temperature relationships in Selangor, Malaysia.” GIS Development.

Burghardt, R., L. Katzschner, S. Kupski, R. Chao and T. Spit (2010). Urban climatic map of Arnhem city.

Carlson, T. N. and A. J. Ripley (1997). “On the relationship between fractional vegetation cover, leaf area index and NDVI.” Remote Sensing Environment 62: 241–252.

Chen, X., H. Zhao, P. Li and Z. Yin (2006). “Remote sensing image-based analysis of the relationship between urban heat island and land use/cover changes.” Remote Sensing of Environment 104(2): 133-146.

Fung, W., K. Lam, J. Nichol and M. Wong (2009). “Derivation of nighttime urban air temperatures using a satellite thermal image.” American Meteorological Society 48: 863-872.

Hung, T., D. Uchihama, S. Ochi and Y. Yasuoka (2006). “Assessment with satellite data of the urban heat island effects in Asian mega cities.” International Journal of Applied Earth Observation and Geoinformation 8: 34-48.

Ibrahim, I., A. Abu Samah and R. Fauzi (2013). “Biophysical factors of remote sensing approach in urban green analysis.” Geocarto International.

Joshi, J. P. and B. Bhatt (2012). “Estimating Temporal Land Surface Temperature Using Remote Sensing: A Study Of Vadodara Urban Area, Gujarat.” International Journal of Geology, Earth and Environmental Sciences 2(1).

JPBD (2002). Detention pond area as part of Open Space.

Kim, Y.-H. and J.-J. Baik (2002). “Maximum urban heat island intensity in Seoul.” American Meteorological Society.

Klysik, K. and K. Fortuniak (1999). “Temporal and spatial characteristics of the urban heat island of Lódz, Poland.” Atmospheric Environment 33(24-25): 3885-3895.

Kubota, T. and D. R. Ossen (n.y.). Spatial characteristics of urban heat island in Johor Bahru City, Malaysia, University Technology Malaysia (UTM): 39-60.

Li, J. (2006). “Estimating land surface temperature from Landsat-5 TM.” Remote Sens. Technol. Appl. 21: 322-326.

Liu, W., C. Ji, J. Zhong, X. Jiang and Z. Zheng (2007). “Temporal characteristics of the Beijing urban heat island.” Theor. Appl. Climatol. 87.

Markham, B. L. and J. L. Barker (1986). “Landsat MSS and TM postcalibration dynamic ranges, exoatmospheric reflectances and at-satellite temperatures.” EOSAT Landsat Tech Notes 1(3-8).

Mega, V. and J. Pedersen (1998). Urban sustainability indicators. Dublin, Ireland.

Meteorology Department. (2012). “Climate.”

Narimah Samat (2006). Applications of Geographic Information Systems in urban land use planning in Malaysia. Taipei International Conference on Digital Earth, Taiwan.

National Aeronautics and Space Administration. (2012). “Landsat 7 Science Data Users Handbook.” from http://landsathandbook.gsfc.nasa.gov/.

Pongrácz, R., J. Bartholy, Z. Dezs and E. Lelovics (n.y.). “Urban heat island effect of large central european cities using satellite measurements of surface temperature.” 1-3.

Qin, Z. and A. Karnieli (2001). “A mono-window algorithm for retrieving land surface temperature from Landsat TM data and its application to the Israel- Egypt border region.” International Journal of Remote Sensing 22(18): 3719-3746.

Qin, Z., A. Karnieli and P. Berliner (2001). “Thermal variation in the Israel-Sinai (Egypt) peninsula region.” Int. Journal Remote Sensing 22(6): 915-919.

Sani, S. (1990). “Urban Climatology in Malaysia: An Overview.” Energy and Buildings 15: 105-117.

Shaharuddin Ahmad and Noorazuan Md Hashim (2007). “Effects of Soil Moisture on Urban Heat

Island Occurrences: Case of Selangor, Malaysia.” Humanity & Social Sciences Journal 2(2): 132-138.

Shaharuddin Ahmad, Noorazuan Md. Hashim and Yaakob Mohd Jani (2009). Fenomena Pulau

Haba Bandar dan isu alam sekitar di Bandaraya Kuala Lumpur. Malaysian Journal of Society and Space.

Sobrino, J. A., J. C. Jimenez-Munoz and L. Paolini (2004). “Land surface temperature retrieval from LANDSAT TM 5.” Remote Sensing of Environment 90: 434–440.

Streutker, D. R. (2003). A study of the urban heat island of Houston, Texas. Ph.D. 3090184, Rice University.

Sun, Q., J. Tan and Y. Xu (2010). “An ERDAS image processing method for retrieving LST and describing urban heat evolution: a case study in the Pearl River Delta Region in South China.” Environ Earth Sci 59: 1047-1055.

United Nation Statistics Division (2012). “Population growth and distribution.”

Wai, N. M., A. Camerlengo and Ahmad Khairi Abdul Wahab (2005). “A study of global warming in Malaysia.” Jurnal Teknologi 42(F): 1-10.

WWF Malaysia (2001). Bring back the birds! Planning for trees and other plants to support wildlife in urban areas.

Xie, H., H. Guan and S. Ytuarte (2005). Heat island of San Antonio, Texas detected by MODIA/AQUA temperature product. Biennial Workshop on Aerial Photography, Videography, and High Resolution Digital Imagery for Resource Assessment, Weslaco, Texas.